On the synthesis and microstructure analysis of high performance MnBi

Cite as: AIP Advances **6**, 125301 (2016); https://doi.org/10.1063/1.4971759
Submitted: 03 October 2016 • Accepted: 21 November 2016 • Published Online: 05 December 2016

Yu-Chun Chen, Simon Sawatzki, Semih Ener, et al.

On the synthesis and microstructure analysis of high performance MnBi

Yu-Chun Chen,[1,a] Simon Sawatzki,[2] Semih Ener,[2] Hossein Sepehri-Amin,[3] Andreas Leineweber,[4] Giuliano Gregori,[5] Fei Qu,[6] Shreyas Muralidhar,[1] Tadakatsu Ohkubo,[3] Kazuhiro Hono,[3] Oliver Gutfleisch,[2] Helmut Kronmüller,[1] Gisela Schütz,[1] and Eberhard Goering[1,a]

[1]*Max Planck Institute for Intelligent Systems, Heisenbergstrasse 3, Stuttgart 70569, Germany*
[2]*Institute of Materials Science, Technische Universitaet Darmstadt, Alarich-Weiss-Strasse 16, Darmstadt 64287, Germany*
[3]*National Institute for Materials Science, 1-2-1 Sengen, Tsukuba 305-0047, Japan*
[4]*Institute of Materials Science, Technische Universitaet Bergakademie Freiberg, Gustav-Zeuner-Strasse 5, Freiberg 09599, Germany*
[5]*Max Planck Institute for Solid State Research, Heisenbergstrasse 1, Stuttgart 70569, Germany*
[6]*Institute of Materials Science, Universitaet Stuttgart, Heisenbergstrasse 3, Stuttgart 70569, Germany*

(Received 3 October 2016; accepted 21 November 2016; published online 5 December 2016)

Highly anisotropic MnBi powder with over 90 wt% low-temperature phase can be prepared using conventional arc-melting and 2 hour-low energy ball milling (BM) followed by magnetic separation. After proper alignment, the purified $Mn_{55}Bi_{45}$($Mn_{45}Bi_{55}$) powder show remarkable magnetic properties: mass remanence of 71(65) Am^2/kg and coercivity of 1.23(1.18) T at 300 K. The nominal maximum energy product of 120 kJ/m^3 is achieved in the purified 2h-BM $Mn_{55}Bi_{45}$ powder, close to theoretical value of 140.8 kJ/m^3. The $Mn_{55}Bi_{45}$($Mn_{45}Bi_{55}$) bulk magnets show the highest volume remanence of 0.68(0.57) T at 300 K, while they were consolidated at 573(523) K by a pressure of 200 MPa for 5 minutes using hot-compaction method. In addition to the observed grain size, the coercivity of the hot-compacted samples at 300 K was found to be strongly related to the amount of metallic Mn and Bi residue at the grain-boundary. Our study proves that the magnetic properties of the $Mn_{45}Bi_{55}$ bulk magnets are stable up to 500 K, and the nominal $(BH)_{max}$ values are still above 40 kJ/m^3 at 500 K showing the potential ability for high-temperature applications. [http://dx.doi.org/10.1063/1.4971759]

I. INTRODUCTION

The rare-earth (RE) permanent magnets have been developed rapidly since the discovery of $SmCo_5$ and $Nd_2Fe_{14}B$ compounds in the sixties and eighties, respectively. Due to their superior magnetic properties, NdFeB-based magnets have been widely used in permanent magnet-based electric machines.[1,2] Unfortunately, the availability and supply of rare earths is particularly precarious. Therefore, RE-free permanent magnets have recently gained considerable attention as they have shown great potential to fill the gap between the energy product of two dominant products in the market, $Ba(Sr)Fe_{12}O_{19}$ and $Nd_2Fe_{14}B$.[3] Among several compounds, the low temperature phase (LTP) of MnBi has been extensively studied because it exhibits several interesting magnetic properties: (i) high magnetocrystalline anisotropy ($K_1 \approx 10^6$ J/m^3)[4,8] and (ii) a very unusual positive temperature coefficient of coercive field (β).[4,6,8] These outstanding features make LTP-MnBi a promising candidate for high temperature applications. Various manufacturing techniques have been employed to achieve

[a]Authors to whom correspondence should be addressed. Electronic mail: chen@is.mpg.de, goering@is.mpg.de

high quality MnBi powder: mechanical grinding,[5] melt-spinning[6] and ball-milling.[4,7,8] Although melt-spun and purified ball-milled powder can contain over 90 wt% LTP, preparation of sintered MnBi bulk magnets with a high level of LTP-MnBi is still a very challenging task.[8,9] First of all, it was found that Mn tends to segregate from MnBi liquid through a peritectic reaction at ~719 K.[6,10] Secondly, the decomposition of LTP-MnBi takes place at ~535 K by eutectic reaction.[8,10] Finally, both MnBi compound and elemental Mn are sensitive to oxygen, meaning that the formation of manganese oxides is practically inevitable.[6,8,9] Therefore, it is necessary to optimize both powder synthesis and consolidation methods in order to develop high performance MnBi-based magnets, which is the aim of this work.

II. EXPERIMENTAL DETAILS

In this study, the MnBi ingots were prepared from Mn pieces (Alfa Aesar, 99.95 %) and Bi granules (Aldrich, ≥ 99.99 %) with designed Mn:Bi atomic ratios of 55:45 and 45:55, via arc-melting in argon atmosphere. The ingots were subsequently annealed at 573 K in vacuum for 1~3 days. The annealed ingots were crushed manually in air and immediately ground into finer powder in a planetary ball mill (BM) at 150 rpm. The ball milling process was completed in hexane under argon atmosphere with hardened steel balls for 2~12 hours at room temperature. In order to maximize the LTP content, the as-milled powders were cleaned by ethanol for the removal of excess hexane, and then purified by magnetic separation for the selection of strong ferromagnetic particles before consolidation.

Because the purified 2h-BM Mn_xBi_{100-x} (x = 45, 55) powders exhibit the highest mass saturation magnetization (M_s) and remanent magnetization (M_r), only they were used for consolidation. To fabricate bulk magnets, the powders were first placed into a cylinder die made of Ni-based alloy and aligned under a perpendicular magnetic field of 1.8 T at room temperature. After pre-alignment, the powder was cold-pressed under a uniaxial pressure of 200 MPa, which was applied parallel to the axis of cylinder die. The aligned Mn_xBi_{100-x} (x = 45, 55) compacts were then consolidated by hot-compaction in vacuum at 473, 523, and 573 K (200, 250, and 300 °C) for 5 minutes, respectively. Throughout hot-compaction process, a uniaxial pressure of 200 MPa was applied parallel to the initial cold compaction direction. In the following, the bulk samples are denoted as $Mn_{55}Bi_{45}$($Mn_{45}Bi_{55}$)-473, -523 and -573 respectively.

The phases and structure of the MnBi samples were characterized by X-ray diffraction (XRD) using both Co and Cu $K\alpha_1$ radiation. Phase contents and cell parameters were determined by whole pattern Rietveld refinement using Topas and crystal structures from the Inorganic Crystal Structure Database. The chemical composition (at.%) was analyzed using inductively coupled plasma optical emission spectroscopy (ICP-OES). Magnetic properties were measured by a superconducting quantum interference device (SQUID) magnetometer. Compaction densities of the bulk samples were determined by Archimedes method and gas pycnometer, which give the same values for all bulk samples. All magnetization curves, $M(H)$, were measured up to 7 T, and the volume magnetization of bulk samples were further evaluated in terms of the corresponding compaction densities (8.6 ~ 8.8 g/cm^3) and demagnetization correction. The demagnetization factor was calculated by the three-dimensional lengths of each sample using the analytic equation given in Ref. 11. Nominal $(BH)_{max}$ values were determined by the value on the second quadrant of B-H curves intersected with the corresponding load lines. The morphology and phases of the samples were examined by scanning electron microscope equipped with energy-dispersive spectrometer (SEM/EDS).

III. RESULTS AND DISCUSSION

Figure 1(a) shows the XRD patterns of the as-milled $Mn_{55}Bi_{45}$ powder as a function of ball milling time. Three phases can be identified from the diffraction patterns, which are LTP-MnBi [$P6_3/mmc$, a = 4.291 Å, c = 6.123 Å], α-Mn [$I\bar{4}3m$, a = 8.921 Å], and Bi [$R\bar{3}m$, a = 4.547 Å, c = 11.872 Å], respectively. It is noted that no high temperature phase (HTP) of MnBi could be found in all powder samples within the detection limit of our XRD measurements. For the $Mn_{55}Bi_{45}$ powders, the intensities of characteristic Bi peaks increase significantly with increasing ball milling time, which

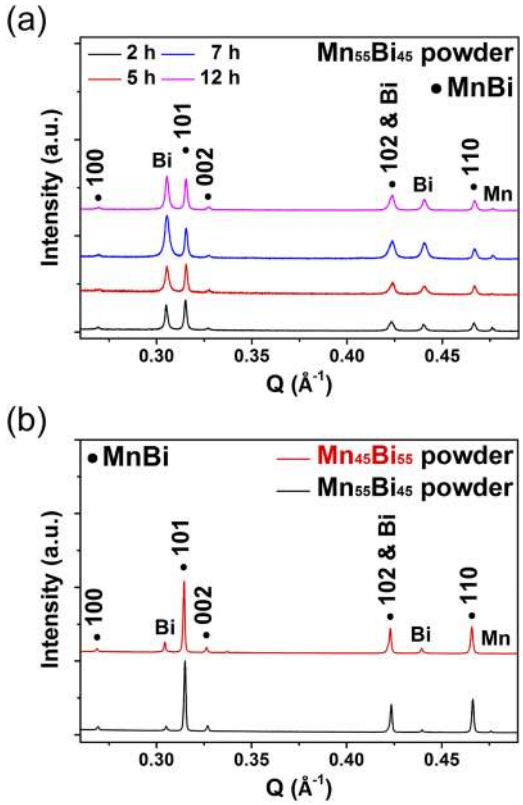

FIG. 1. Room temperature XRD patterns: (a) as-milled $Mn_{55}Bi_{45}$ powder for different ball-milling times. (b) purified $Mn_{55}Bi_{45}$ and $Mn_{45}Bi_{55}$ powder (2h-BM).

indicate the decomposition of the LTP-MnBi during ball milling procedure. Rietveld analysis shows that the LTP content of as-milled $Mn_{55}Bi_{45}$ powders goes down from 49 wt.% (for 2h-BM) to 29 wt.% (for 7h-BM), while the Bi content increases from 38 wt.% (for 2h-BM) to 70 wt.% (for 7h-BM). The increase in Bi residue is also observed by the chemical analysis (ICP-OES) from which, for example, the 2h- and 7h-BM purified $Mn_{55}Bi_{45}$ powder contain 45.6 and 54.7 at.% Bi, respectively. In contrast, the $Mn_{45}Bi_{55}$ powders always have high level of Bi (> 52 at.%) without obvious systematic variation in atomic ratios (not shown here). Figure 1(b) proves that the fraction of LTP in the 2h-BM powders can be further enriched through magnetic separation. The Rietveld analysis reveals that the LTP content increases dramatically, for example, from 49 wt.% for as-milled $Mn_{55}Bi_{45}$ powders to 90 wt.% for corresponding purified ones. Conversely, a significant decrease is observed in the peak intensities of the non-ferromagnetic Bi and Mn peaks. However, we found that long-term milled powders are not easily purified, therefore only purified 2h-BM powder was selected for consolidation. Furthermore, a relatively high fraction of secondary phase Bi (~6 wt.%) is always present, even for the finely purified powders as can be seen in Fig. 1(b). It is quite usual to have decomposed phases at the surface of ball milled particles, therefore we suggest that part of the powders should be covered by a thin Bi-rich layer. In order to maximize the magnetic properties (i.e. wt% of LTP-MnBi), powders were always purified by magnetic separation before consolidation. It is noted that the actual Mn:Bi atomic ratios of the purified 2h-BM $Mn_{55}Bi_{45}$and $Mn_{45}Bi_{55}$ powder are 53:47 and 46:54, which are slightly different from the designed values. Additionally, we emphasize that the SQUID values are more reliable than the phase contents given by Rietveld refinement due to the large difference in X-ray scattering factors of Mn and Bi elements.

The room temperature M(H) curves are shown in Fig. 2 for the purified $Mn_{55}Bi_{45}$ and $Mn_{45}Bi_{55}$ powders. All powders were aligned with resin under 2 T magnetic field. It is obvious that the M_s and M_r ratios of purified $Mn_{55}Bi_{45}$ powders drop rapidly with increasing milling time. Although long-term BM can slightly enhance the coercivity, it reduces magnetization drastically and even leads to a

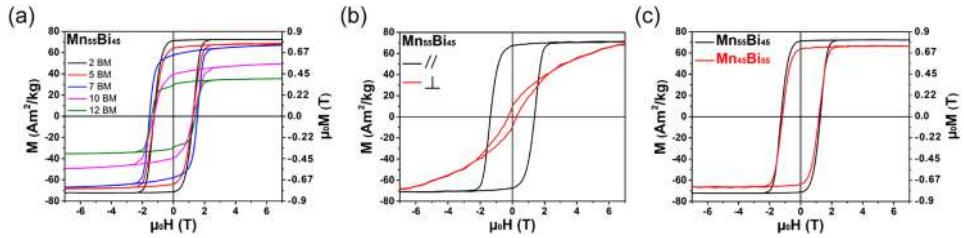

FIG. 2. M(H) curves of purified powder at 300 K: (a) $Mn_{55}Bi_{45}$ milled for different time. (b) 2h-BM $Mn_{55}Bi_{45}$ measured parallel (⊥) and perpendicular (//) to the alignment directions. (c) purified 2h-BM $Mn_{55}Bi_{45}$ and $Mn_{45}Bi_{55}$.

kink in the low field range for 12h-BM powder. The drop in magnetization indicates decomposition of LTP-MnBi. Figure 2(b) shows the M(H) curves of 2h-BM $Mn_{55}Bi_{45}$ powder measured parallel and perpendicular to the alignment direction at 300 K, which demonstrates that the aligned powder samples are highly anisotropic. Similar trends were found for the $Mn_{45}Bi_{55}$ series (not shown here). In agreement with Ref. 12 and 13, the SQUID measurements reveal that $Mn_{55}Bi_{45}$ series always exhibits larger M_r and M_s than those of $Mn_{45}Bi_{55}$ samples after identical preparation procedure (see Fig. 2(c)). The highest magnetic properties obtained from the finely purified 2h-BM $Mn_{55}Bi_{45}$($Mn_{45}Bi_{55}$) powder are M_r of ~71(65) Am^2/kg, M_s(7T) of ~72.5(68) Am^2/kg and μ_0H_c of ~1.23(1.18) T at 300 K. The LTP content of the purified 2h-BM $Mn_{55}Bi_{45}$ powder is estimated to be over 90 wt% compared to the theoretical prediction of $M_{s,LTP}$ (80 Am^2/kg).[12] To our knowledge, the M_r of ~71 Am^2/kg is the highest reported value for ball-milled MnBi powder so far.[4,7,8] The volume magnetization of the purified 2h-BM $Mn_{55}Bi_{45}$ powder was further evaluated by theoretical density of LTP-MnBi (8.9 g/cm^3),[4,8] giving μ_0M_r = 0.79 T and μ_0M_s = 0.81 T. Combined with the observed coercivity of 1.23 T, the nominal $(BH)_{max}$ of this purified $Mn_{55}Bi_{45}$ powder reaches 120 kJ/m^3, which is close to the theoretical prediction of 140.8 kJ/m^3.[8,14] Although the μ_0M_r of our powder is slightly lower than that of reported value (74 Am^2/kg) in Ref 8, it is noted that our powder was pre-aligned under 2 T and then measured with a field of 7 T. Nevertheless, we have to emphasize that the purified 2h-BM $Mn_{55}Bi_{45}$($Mn_{45}Bi_{55}$) powder usually shows M_s(7T) of 70(66) ±2 Am^2/kg. It is our experience that the ingot quality has a profound influence on the magnetic performance of the powder, including M_s and $(BH)_{max}$. Therefore, it is crucial to mix metallic Mn and Bi homogeneously during arc-melting process in order to obtain high performance powders.

Figure 3 compares the M(H) curves of the $Mn_{55}Bi_{45}$ and $Mn_{45}Bi_{55}$ magnets compacted at 473, 523, 573 K, which were measured along the pre-alignment direction at 300 K. The highest volume magnetization is observed in $Mn_{55}Bi_{45}$-523 and $Mn_{45}Bi_{55}$-573, respectively. In contrast to the starting purified powders, the $Mn_{45}Bi_{55}$ bulk series exhibits higher magnetic performance compared to the $Mn_{55}Bi_{45}$ bulk one, namely higher volume fraction of LTP-MnBi (see Table I for detailed information). This difference is actually caused by removal of excess Bi from bulk samples because we observed that the compacts and the inner shell of the steel die were covered by many tiny Bi-rich fragments (> 98 at.% Bi by ICP-OES analysis) after hot-compaction process. Due to the low Bi melting point of 545 K close to the sintering temperatures, the liquid Bi from residue or decomposition of LTP was extruded out during consolidation.[8,10] Conversely, the melting point of Mn is rather high (1518 K), so most of the excess Mn is left inside the microstructure.[6,10] As a result, the actual Mn:Bi atomic ratios of bulk samples differ a lot from the designed values and those of starting powders (see Table I). It is noted that both $Mn_{45}Bi_{55}$-523 and $Mn_{45}Bi_{55}$-573 contain excess of Mn even though they were prepared by Bi-rich powders. Among these specimens, $Mn_{45}Bi_{55}$-573 shows μ_0M_r = 0.68 T and μ_0M_s (7T) = 0.79 T at 300 K, which are the highest magnetization values reported for MnBi sintered magnets so far.[4,8] Compared to the starting powders, the μ_0M_r and μ_0M_s values of the $Mn_{45}Bi_{55}$-573 bulk samples decrease slightly by 6% and 4% respectively. However, all hot-compacted samples show relatively low coercivity (≤ 0.31 T) at 300 K in comparison with the previously published work.[4,8] To clarify this issue, the microstructure of the bulk samples was examined by SEM characterization. Because the SQUID results show that $Mn_{45}Bi_{55}$ magnets exhibit better magnetic performance at different temperatures, the following discussions will mainly focus on them.

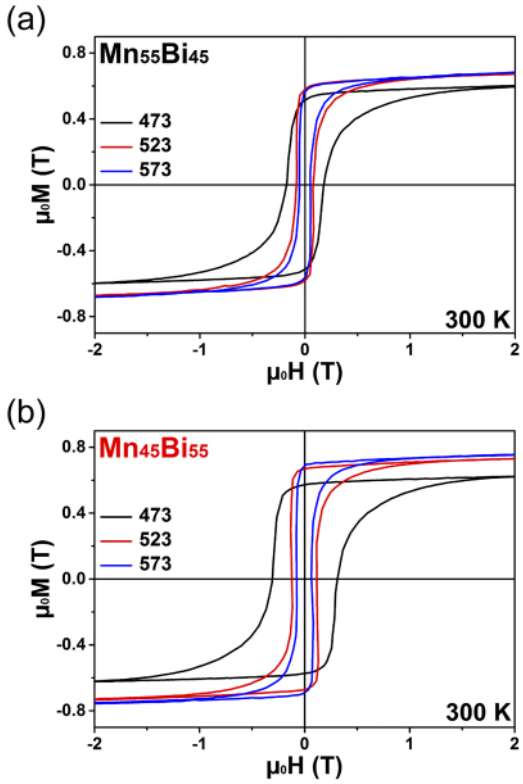

FIG. 3. M(H) curves of (a) $Mn_{55}Bi_{45}$ and (b) $Mn_{45}Bi_{55}$ magnets at 300 K.

The backscattered electron (BSE) images of $Mn_{45}Bi_{55}$ powders and three bulk magnets are shown in Fig. 4. Figure 4(a) reveals that the particle size of 2h-BM powder ranges from 0.5 to 8 μm with average size less than 3 μm. As shown in Figs. 4(b)–(d), three phases [α-Mn (black), Bi (white) and LTP-MnBi (gray)] can be distinguished in the bulk samples, which are confirmed by EDS mapping (not shown here). In addition to three main phases, the grain boundary between neighboring LTP grains clearly shows a different phase contrast; the EDS line-scan analysis indicates that the grain boundary region is rich in Mn (~54 at.%) with a tiny amount of oxygen. BSE images suggest that some grains are elongated along alignment direction with length longer than 15 μm, therefore significant grain growth indeed occurred during the consolidation. We also analyzed the grain size distribution in these bulk samples, and it was found that their grain size distribution looks very similar. But, the number of very large grains (length >18 μm) slightly increases as the consolidation temperature goes up. Because single domain size of LTP-MnBi is ~ 0.5 μm at 300 K,[14,15] the small measured coercive field of our bulk samples can be partially understood due to the existence of the larger grains observed here. This assumption is consistent with the reported relation between grain (or particle) size and $\mu_0 H_c$ values in nanocrystalline thin films[16] and powders.[17] Specifically, the experimental

TABLE I. Chemical compositions and room-temperature magnetic properties of bulk magnets.

Samples	Mn [at.%]	Bi [at.%]	$\mu_0 H_c$ [T]	$\mu_0 M_r$ [T]	$\mu_0 M_s$ [T]
$Mn_{45}Bi_{55}$-473	45.0	55.0	0.31	0.57	0.65
$Mn_{45}Bi_{55}$-523	51.5	48.5	0.14	0.67	0.77
$Mn_{45}Bi_{55}$-573	52.6	47.4	0.08	0.68	0.79
$Mn_{55}Bi_{45}$-473	54.4	45.6	0.18	0.51	0.64
$Mn_{55}Bi_{45}$-523	57.8	42.2	0.08	0.57	0.71
$Mn_{55}Bi_{45}$-573	59.7	40.3	0.05	0.56	0.73

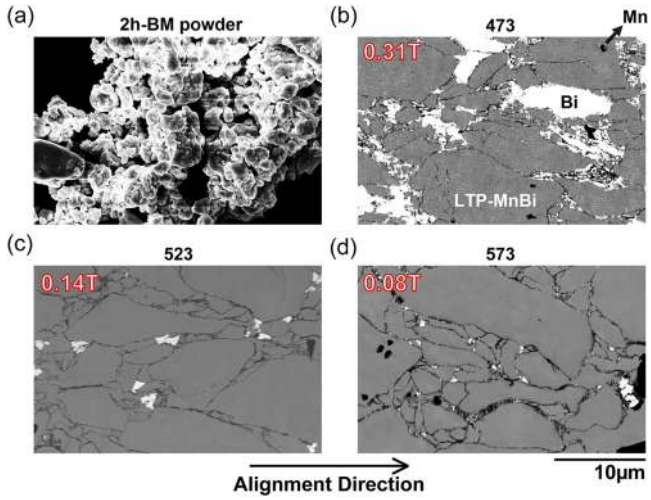

FIG. 4. BSE images of $Mn_{45}Bi_{55}$ (a) 2h-BM powders and (b, c, d) bulk magnets. The value on the top-left corner in each micrograph of the bulk samples refers to the observed coercive fields ($\mu_0 H_c$). The grains were particularly elongated along the alignment direction (roughly horizontal).

data in Ref. 17 show that MnBi powders with diameter of 20 μm exhibit $\mu_0 H_c$ of ~ 0.5 T, which is slightly larger than that of $Mn_{45}Bi_{55}$-473. Therefore, we suggest that the observed low coercive fields should be related to the domain wall movement in the large grains.

The area fractions of three phases (MnBi, α-Mn, and Bi) of the compacted samples were further determined from randomly selected surface area (80 μm × 80 μm). The data in Table II suggest that bulk magnets with more Bi residue have higher coercive field. This tendency can be explained by considering Bi as decoupling layer between LTP grains. Because metallic Bi is diamagnetic material, the LTP-MnBi grains surrounded by thicker Bi area have better magnetic decoupling from others (i.e. $Mn_{45}Bi_{55}$-473 shows the largest $\mu_0 H_c$). Furthermore, the $Mn_{55}Bi_{45}$ bulk series exhibits even lower coercivity because less Bi and a relatively high amount of antiferromagnetic α-Mn is embedded inside the microstructure (not shown here). Theoretically, the exchange coupling between two magnetic phases is considered as a short-range interaction. It is clear that better magnetic decoupling should be achieved between either LTP-MnBi grains or LTP-MnBi/α-Mn phases as the amount of Bi residue increases.

The changes of magnetic properties of $Mn_{45}Bi_{55}$ hot-compacted magnets are shown in Fig. 5 as a function of measuring temperature. Among these three samples, $Mn_{45}Bi_{55}$-573 exhibits the highest magnetization (both $\mu_0 M_r$ and $\mu_0 M_s$) within measuring temperatures, which decreases from 0.68 T and 0.79 T at 300 K to 0.56 T and 0.63 T at 500 K, respectively. Grain misalignment usually causes a drop in the remnant magnetization of bulk magnets. SQUID curves indicate that all $Mn_{45}Bi_{55}$ magnets are highly textured (not shown here), and the M_r/M_s ratios are all above 0.86 within the measuring temperature range (300 ~ 500 K). However, the largest temperature-dependent coercive fields are found in $Mn_{45}Bi_{55}$-473, which increases from 0.31 T at 300 K to 2.1 T at 500 K. Therefore, the highest nominal $(BH)_{max}$ value of $Mn_{45}Bi_{55}$ series at 300 K is 46.1 kJ/m^3 found in $Mn_{45}Bi_{55}$-473. Although the highest $(BH)_{max}$ value in this study is lower than the reported value of 61.6 kJ/m^3 in

TABLE II. Area fraction of three phases in the microstructure of $Mn_{45}Bi_{55}$ bulk samples.

Samples	MnBi [area %]	α-Mn [area %]		Bi [area %]	$\mu_0 H_c$ [T]	$\mu_0 M_s$ [T]
		Residue	Grain-boundary			
$Mn_{45}Bi_{55}$-473	78.6	2.6	1.8	17	0.31	0.65
$Mn_{45}Bi_{55}$-523	83.5	3.3	7.8	5.4	0.14	0.77
$Mn_{45}Bi_{55}$-573	89.4	1.9	7.8	0.9	0.08	0.79

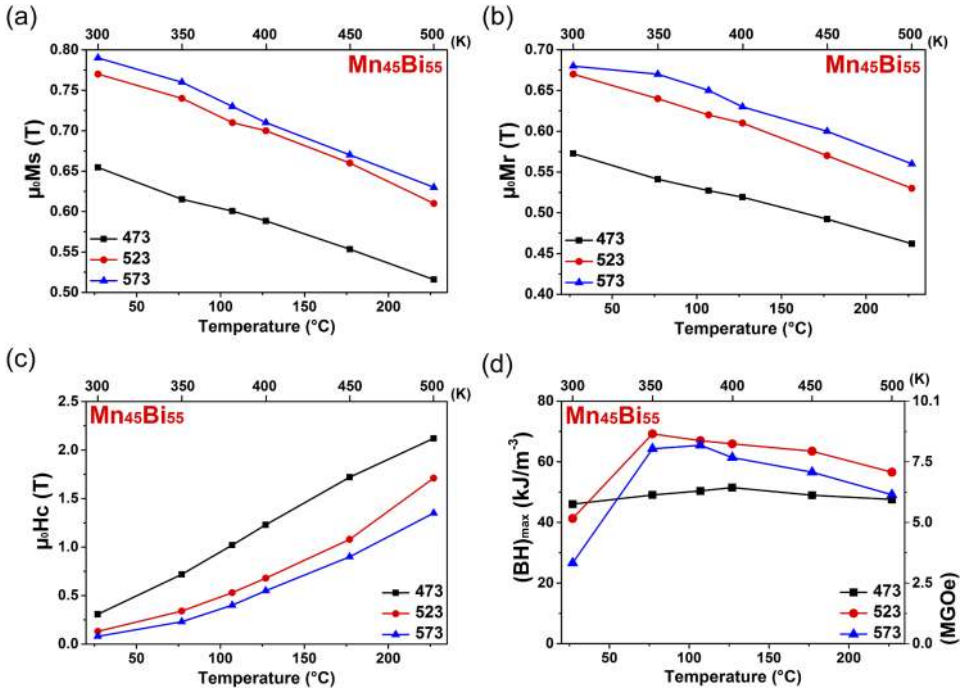

FIG. 5. Temperature-dependent magnetic properties of $Mn_{45}Bi_{55}$ bulk magnets: (a) volume saturation magnetization, (b) volume remanent magnetization, (c) coercive field and (d) $(BH)_{max}$ values at different temperatures (measured along alignment direction).

Ref. 8, it is higher compared to that of commercial ferrite or alnico 5 magnets. We also note that the nominal $(BH)_{max}$ of all $Mn_{45}Bi_{55}$ samples is above 40 kJ/m^3 at 500 K, which is higher than experimental $(BH)_{max}$ of $Nd_2Fe_{14}B$ (15.8 kJ/m^3).[14,15] Furthermore, it was found that all $Mn_{45}Bi_{55}$ and $Mn_{55}Bi_{45}$ bulk samples retain the same magnetic properties after one-day heating at 500 K under inert atmosphere. This evidence strongly suggests that LTP-MnBi can be a good candidate for high temperature applications, while the proper surface coating is carried out to prevent oxidation problem.

IV. CONCLUSION

The LTP-MnBi powder with remarkable magnetic properties (M_r = 71 Am^2/kg and nominal $(BH)_{max}$ of 120 kJ/m^3 at 300 K) can be achieved using conventional ball milling followed by magnetic separation. Bulk magnets with high saturation and remanent magnetization can be fabricated by fast hot-compaction method. The SEM study suggests that the bulk samples with high fraction of Bi exhibit larger coercive fields. In order to enhance the coercivity of hot-compacted MnBi magnets, it is necessary to reduce the grain size and amount of Mn residue. Detailed microstructure and thermodynamic analysis is ongoing to understand the coercive mechanism of MnBi bulk magnets. It is noted that the $(BH)_{max}$ values of $Mn_{45}Bi_{55}$ magnets is still above 40 kJ/m^3 at 500 K, which is higher than that of $Nd_2Fe_{14}B$ (15.8 kJ/m^3). Our results proved that LTP-MnBi based materials can fill the gap of energy products between the best ferrite and Nd-Fe-B magnets.

ACKNOWLEDGMENTS

The authors gratefully acknowledge the support of the Deutsche Forschungsgemeinschaft for the project HPPMSNG and German federal state of Hessen for the program LOEWE RESPONSE, respectively. In particular, we would like to thank the valuable discussions with Prof. Takao Suzuki and Prof. George Hadjiapanayis.

[1] M. J. Kramer, R. W. McCallum, I. A. Anderson, and S. Constantinides, J. Min. Met. Mater. Soc. **64**, 752 (2012).
[2] O. Gutfleisch, M. A. Willard, E. Brück, C. H. Chen, S. G. Sankar, and J. P. Liu, Adv. Mater. **23**, 821 (2011).
[3] J. M. D. Coey, Scripta Mater. **67**, 524 (2012).
[4] N. V. R. Rao, A. M. Gabay, and G. C. Hadjipanayis, J. Phys. D: Appl. Phys. **46**, 062001 (2013).
[5] E. Adams, W. M. Hubbard, and A. M. Syeles, J. Appl. Phys. **23**, 1207 (1952).
[6] Y. B. Yang, X. G. Chen, S. Guo, A. R. Yang, Q. Z. Huang, M. M. Wu, D. F. Chen, Y. C. Yang, and J. B. Yang, J. Magn. Magn. Mater. **330**, 106 (2013).
[7] J. B. Yang, K. Kamaraju, W. B. Yelon, W. J. James, Q. Cai, and A. Bollero, Appl. Phys. Lett. **79**, 1846 (2001).
[8] J. Cui, J. P. Choi, E. Polikarpov, J. Darsell, N. Overman, M. Olszta, D. Schreiber, M. Bowden, T. Droubay, M. J. Kramer, N. A. Zarkevich, L. L. Wang, D. D. Johnson, M. Marinescu, I. Takeuchi, Q. Z. Huang, H. Wu, H. Reeve, N. V. Vuong, and J. P. Liu, J. Phys.: Condens. Matter. **26**, 064212 (2014).
[9] Y.-C. Chen, G. Gregori, A. Leineweber, F. Qu, C.-C. Chen, T. Tietze, H. Kronmüller, G. Schütz, and E. Goering, Scripta Mater. **107**, 131 (2015).
[10] K. Oikawa, Y. Mitsui, K. Koyama, and K. Anzai, Mater. Trans. JIM **52**, 2032 (2011).
[11] A. Aharoni, J. App. Phys. **83**, 3422 (1988).
[12] C. Chinnasamy, M. M. Jasinski, A. Ulmer, W. Li, G. Hadjipanayis, and J. Liu, IEEE Trans. Magn. **48**, 3641 (2012).
[13] J. Cui, J.-P. Choi, E. Polikarpov, M. E. Bowden, W. Xie, G. Li, Z. Nie, N. Zarkevich, M. J. Kramer, and D. Johnson, Acta Mater. **79**, 374 (2014).
[14] J. Park, Y.-K. Hong, J. Lee, W. Lee, S.-G. Kim, and C.-J. Choi, Metal **4**, 455 (2014).
[15] H. Kronmüller, J. B. Yang, and D. Goll, J. Phys.: Condens. Matter **26**, 064210 (2014).
[16] T. Hozumi, P. LeClair, G. Mankey, C. Mewes, H. Sepehri-Amin, K. Hono, and T. Suzuki, J. App. Phys. **115**, 17A737 (2014).
[17] F. D. Luborsky, J. App. Phys. **32**, S171 (1961).